Journal of the Serbian Chemical Society
JSCS-info@shd.org.rs • www.shd.org.rs/JSCS

ACCEPTED MANUSCRIPT

Journal of the Serbian Chemical Society
JSCS-info@shd.org.rs • www.shd.org.rs/JSCS
J. Serb. Chem. Soc. **00(0)** 1-15 (2024)
JSCS–12633
Original scientific paper
Published DD MM, 2024

Preparation, characterization and evaluation of nano manganese dioxide coated on alumina as a new adsorbent for the effective removal of phenol from aqueous samples

SAYED ZIA MOHAMMADI[1], FARIDEH MOUSAZADEH[2]*, LEILA SALAJEGHEH-TEZERJI[1], BATOUL LASHKARI[3], ELINA BANI-ASADI[2]

[1]Department of Chemistry, Payame Noor University, Tehran, Iran, [2]School of Public Health, Bam University of Medical Sciences, Bam, Iran, and [3]Department of New Materials, Institute of Science and High Technology and Environmental Sciences, Graduate University of Advanced Technology, Kerman, Iran

(Received 21 October 2023; revised 14 November 2023; accepted 6 April 2024)

Abstract: An effective sorbent as title nano manganese dioxide coated on alumina (NMO/Al) nanocomposite was prepared as an economical adsorbent in the present study. To this end, morphological, chemical, and surface characteristics of NMO/Al were determined through various techniques. The NMO/Al nanocomposite could be thus separated effortlessly from water samples using a filter paper and then, the removal of phenol from the wastewater samples was evaluated. Accordingly, various empirical parameters affecting this removal including pH, ionic strength, time, temperature, and phenol concentration were examined. In order to investigate the adsorption equilibrium, Langmuir, Freundlich, and Temkin equations were utilized and since that the Langmuir adsorption model had a higher correlation coefficient (R^2) indicating better fit to the adsorption characteristics. Various kinetic models were employed to evaluate the adsorption kinetics of phenol on the NMO/Al nanocomposite. Based on the results, the Elovich model exhibited the best fit with a sorption capacity of 21.34 mg/g. Additionally, the adsorbed phenol was desorbed from the NMO/Al surface by using ethanol and with high efficiency, and then the NMO/Al nanocomposite was used again to remove phenol. The results showed that the NMO/Al nanocomposite could be reused for more than five cycles. Based on the findings, the phenol adsorption process from wastewater using NMO/Al nanocomposite is considered an efficient adsorption approach in a large-scale adsorption system.

Keywords: nano manganese dioxide; alumina; nanocomposite; phenol; removal.

* Corresponding author. E-mail: faridehmousazadeh1398@gmail.com
https://doi.org/10.2298/JSC231021042M

INTRODUCTION

With the growing pace of industrial development, pollution of water resources has become significantly hazardous throughout the world. There are various applications for phenol, such as in medicine, pesticides, explosives, garments, petrochemicals, and other fields. However, the usage of phenol generates a significant amount of toxic, carcinogenic, and difficult-to-degrade phenol wastewater, which has severe consequences for human health and the environment. Indeed, the treatment of phenol wastewater is of paramount importance.[1] The United States Environmental Protection Agency has classified phenol as a critical pollutant due to its high toxicity and its widespread contamination of water resources.[2] Long-term exposure to phenol can have adverse effects on human organs, including the possibility of causing cancer. As a result, the recommended discharge limit for phenol in surface water is less than 1 μg/L.[3] Therefore, the treatment of phenol wastewater is an urgent and critical issue.[4] To address this issue, various physical, chemical, and biological processes have been employed for the removal and/or recovery of phenol. Some of these processes include biosorption, electro-fenton, extraction with solvent, electrodialysis, degradation, biodegradation, membrane methods, and sorption.[6-10] But most of the mentioned techniques are relatively expensive or had been reported costly in treating secondary toxic sludge. Compared to other processes, absorption is still economically the most profitable method due to its advantages such as simple design, ease of adsorbent regeneration, adsorption capacity, and minimum capital investment requirements.

Different adsorbents such as organic framework,[2] activated persulfate,[1,4] bimetallic/carbon nanocomposite,[5] ZnO nanoparticles,[6] nanocomposites,[7] Granulated cork,[8] modified SiO_2,[9] magnetic activated carbon -cobalt nanoparticles,[10] non-living Phanerochaete,[11] kaolin/γ-Fe_2O_3,[12] magnetic diatomite[13] and so on were used for removal of phenol. Alumina (Al_2O_3) is a suitable adsorbent material for treatment of effluents due to its good porosity, and thermal stability, that making it an economical alternative.[14] Moreover, alumina is naturally available and can be easily obtained through chemical reaction from $Al(OH)_3$. To further improve its adsorption efficiency, alumina can be modified through physical or chemical treatment, which increases the density of active sites on its surface. While alumina is a sorbent with many benefits, it can be further improved for enhanced adsorption potential toward organic molecules by modifying it with metals, metal oxides, or other substances. Additionally, due to Lewis acid and base groups on the surface of Al_2O_3, strong interactions between the surface of alumina and metal oxides have been formed and therefore the absorption and catalytic properties of alumina was improved.[15] Previously, manganese dioxide coated on alumina was used to remove arsenic and fluoride ions from water samples, but based on our knowledge this adsorbent has not been

used to remove the phenol and in addition, the method of coating manganese dioxide on alumina in the present work is different from the method of previous works.[16,17]

In the present study, nano manganese dioxide coated on alumina nanocomposite (NMO/Al) with high absorption capacity was successfully prepared. The NMO/Al nanocomposite was employed for the removal of phenol under various experimental conditions. Furthermore, the impacts of initial adsorbate concentration, contact time, pH, and sorbent capacity on the phenol removal were assessed.

EXPERIMENTAL

Reagents and equipment

Phenol was obtained from Merck, Germany (Darmstadt) and was used to prepare a 1000.0 mg/L solution in DIW (deionized water). Al_2O_3 (0.063-0.2 mm) (Merck) was used for the preparation of NMO/Al nanocomposite. The absorbance of phenol was measured using a Varian Cary 50 Scan UV-Visible (UV-Vis) spectrophotometer with quartz cells. Phenol absorbance values were measured at 270 nm, which is the wavelength of maximum absorbance. pH was measured by Metrohm pH-meter (Model 713) with a combined glass electrode (Metrohm). The solutions were agitated by IKA stirrer model KS (Staufen; Germany). After adsorbing of phenol from sample solution, the NMO/Al was recovered by a filter paper.

X-ray diffraction (XRD) was performed using a Bruker D8 ADVANCE diffractometer with copper/K-alpha (Cu/Kα) radiation. The microstructure of NMO/Al was observed using a scanning electron microscope (SEM; Cam Scan MV2300; Cambridge; UK). X-ray photoelectron spectroscopy (XPS) was conducted using an AXIS-Ultra device from Kratos Analytical Ltd. with monochromatic aluminum (Al)/Kα radiation (225 W; 15 mA; 15 kV). Fourier transform infrared (FT-IR) spectra were recorded using a Brucker Tensor 27 spectrometer with the KBr wafer technique.

Preparation of NMO/Al

Manganese dioxide was precipitated onto alumina in an aqueous solution through a reductive reaction, as shown in equation (1):[18]

$$2KMnO_4 + 8HCl \rightarrow 2MnO_2 + 2KCl + 3Cl_2 + 4H_2O \quad (1)$$

To perform this reaction, 4.0 g of potassium permanganate was added to 50 mL of deionized water contain 4.0 g of alumina. Then, 8 mL of concentrated HCl was added dropwise to the mixture while continuously stirring and heating it on a hot plate at 90 °C. The stirring and heating process were continued for 1 hour. The coated alumina was then filtered, washed with boiling water, dried in an oven at 80 °C for 6 hours, and stored in a bottle for later use.

Phenol removal method

To evaluate the ability of NMO/Al nanocomposite for phenol removal, the tests were done in a batch method at 25°C and to increase the accuracy of each test, it was repeated 3 times. To determine the highest yield of NMO/Al nanocomposite for phenol removal, the effective parameters on the phenol removal such as contact time, solution temperature, solution pH, ionic strength and phenol concentration were assessed and optimized.

For this assesses, 0.05 g of NMO/Al was added to a solution containing phenol. The Erlenmeyer flasks were agitated (340 rpm) using an IKA stirrer model KS for a certain period

of time. After agitation, filter paper was used to separate the NMO/Al from the solution, and then the absorbance of the solution under the filter was measured using an UV-Vis (270 nm).

For assesses of the initial concentration of phenol onto phenol removal, the concentration range of 50 to 150 mg/L at pH 7 was assessed. For this purpose, a concentration of 50 mg/L was used to examine the adsorption under other conditions.

The effect of solution pH on the phenol removal was examined over a pH range of 2 to 9. Furthermore, adsorption thermodynamic was assessed at various temperatures (275-309 K). Various concentrations of sodium chloride (NaCl solution) (ranging from 0 to 0.5 mol/L) were assessed to investigate the salting effect on the phenol removal. It should be noted that, the percentage removal (Re%) was calculated using Equation 2.

$$Re\% = \frac{C_0 - C_t}{C_0} \times 100 \quad (2)$$

where C_0 (mg/L) refers to the initial concentration and C_t (mg/L) refers to the amount of phenol at time t.

The amount of phenol adsorbed by the NMO/Al nanocomposite after time t (q_t, mg/g) was calculated using Equation 3:

$$q_t = \frac{(C_0 - C_t)\,V}{W} \quad (3)$$

where C_0 and C_t have the same definitions as before, V(L) refers to the volume of solution, and W(g) refers to the mass of the adsorbent.

Assesses of desorption

Similar to the adsorption tests, NMO/Al (0.05 g) was added to a phenol solution (50 mg/L) with a contact time of 60 minutes at 298 K. After this, filter paper was used to separate the NMO/Al loaded with phenol from the solution, and in the following, DIW used to wash and remove any unabsorbed traces of phenol.

The consumed NMO/Al nanocomposite that saturated with phenol was regenerated using ethanol (10 mL) that added to the phenol- saturated NMO/Al and stirred for 30 minutes at 298 K and 340 rpm. Once desorption was completed, the adsorbent was separated, washed with DIW and for the next use, placed in an oven with a temperature of 378 K to dry. To assess the reusability of the NMO/Al, the absorption and desorption process was repeated 5 times.

RESULTS AND DISCUSSION

NMO/Al characterization

The functional groups on the surfaces of alumina and NMO/Al were assessed by using FT-IR spectroscopy. FT-IR spectra (shown in Fig. 1a) were recorded using the KBr wafer technique over a range of 400-4000 cm^{-1}. To prepare the wafers, a mixture of 1 mg of the sample and 100 mg of KBr was used.

The absorption bands observed at 3447 and 1617 cm^{-1} in the FT-IR spectra are attributed to the stretching and bending vibrations of adsorbed water molecules (ν(OH)), respectively. The broad peak at 811 cm^{-1} is caused by the Al-O vibration.[19] The appearance of new bands at 458, 517, and 711 cm^{-1} can be attributed to the Mn-O vibration, which makes the NMO/Al nanocomposite spectrum different from the alumina spectrum. Therefore, the presence of MnO_2 on the surface of alumina was confirmed.

The crystalline structure of the NMO/Al nanocomposite was characterized by XRD analysis (as shown in Fig. 1b). The present diffraction peaks at 2θ values of 32.5°, 37.6°, 39.6°, 45.9°, 61.1°, and 67.1°, could be related to crystal plates (220), (311), (222), (400), (511), and (440), respectively. These peaks suggest the cubic structure of γ-Al_2O_3 (JCPDS Card no. 01-1303). The calculations made using the Debye- Scherrer equation showed that the size of the γ-Al_2O_3 to be 27 nm.

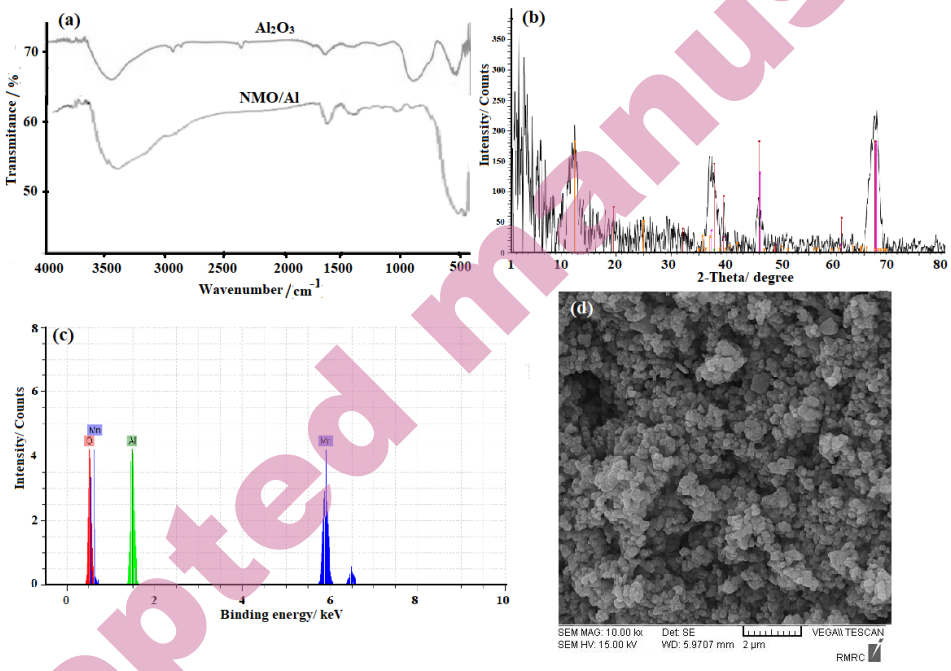

Fig. 1. (a) FT-IR spectra of Al_2O_3 and NMO/Al, (b) XRD of NMO/Al, (c) XPS of NMO/Al and (d) SEM of NMO/Al.

Furthermore, as shown in Fig. 1b, the present diffraction peaks at 2θ values of 12.9°, 18.3°, 28.8°, 37.7°, 42.1°, 49.9°, 56.44°, 60.26°, 69.7°, 71.3°, and 73.7°, could be related to crystal plates (110), (200), (310), (211), (301), (411), (600), (521), (541), (222), and (730), respectively. With respect to these results, the successful synthesis of tetragonal crystalline α-MnO_2 was confirmed (standard card JSPDF 44-0141).[20]

Also, X-ray photoelectron spectroscopy (XPS) was used for assesses the chemical compositions of the NMO/Al nanocomposite. The presence of Al, Mn, and O elements in the NMO/Al nanocomposite was confirmed by using XPS of NMO/Al (Figure 1c). Quantitative data analysis of the XPS spectra yielded weight ratios of 21.96% for Al, 22.81% for Mn, and 55.23% for O in the NMO/Al nanocomposite.

The morphological features of the NMO/Al nanocomposite showed in Figure 1d. The SEM images of NMO/Al reveal that it has a spherical shape. The porous microstructure of NMO/Al suggests that it has a large surface area, therefore, it has a good potential to be used as an adsorbent with a high adsorption capacity of pollutants.

The effect of pH

A very important factor in the adsorption process is the pH of the solution because the functional groups on the surface of the adsorbent as well as the chemical structure of the phenol molecule could be affected by pH of solution.[21,22] So, the effect of pH on the removal percentage (Re%) of phenol was evaluated in this study over a pH range of 2-9 (Fig. 2a). The results showed that the maximum sorption of phenol occurred in the pH range of 7-9.

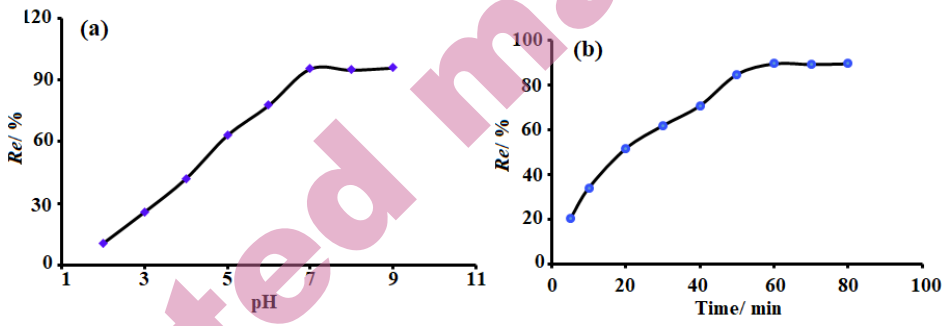

Fig. 2. (a) The impact of pH on the adsorption of phenol onto the NMO/Al. Conditions: 25 mL phenol 50.0 mg/L. Agitation time: 60 minutes. Agitation velocity: 340 rpm. NMO/Al, 0.05 g and (b) The impact of contact time on the adsorption of phenol onto the NMO/Al. Conditions have been similar to Figure 2(a) except to the agitating time.

The acid dissociation constant (pKa) value for phenol was 9.89; therefore, at pHs less than pKa, phenol molecules exist in non-dissociated state, and the reason for phenol adsorption can be attributed to π-π dispersion interaction, physical adsorption, hydrogen bonding, and hydrophobic interaction. [23] With respect to the obtained results, other experiments for removal of phenol were done at pH 7.

The assesses of contact time and initial concentrations

The impacts of initial concentration and contact time on the Re% of phenol could be showed in Fig. 3 and Fig. 2b, respectively.

According to Figure 2b, the phenol adsorption enhances quickly in the early 30 min and reaches balance at 60 min. With the start of the adsorption process, phenol molecules gradually occupy the active sites on the NMO/Al surface, in the next step, phenol molecules must be transferred from the bulk solution to the active sites on the surface of the NMO/Al nanocomposite. This gradual diffusion would decline the sorption level of phenol after 30 min.

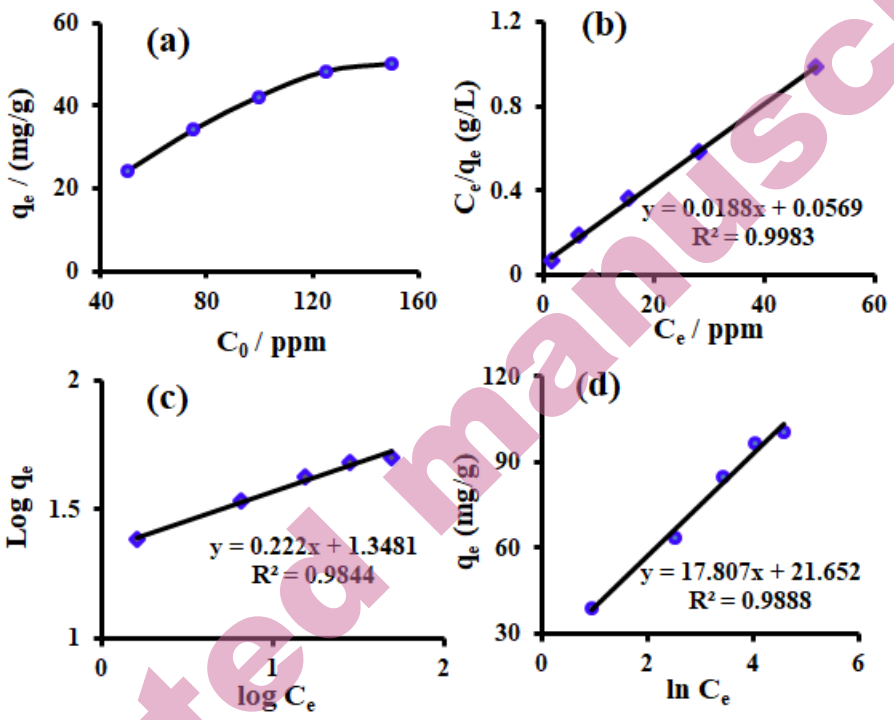

Fig. 3. (a) The impact of initial concentrations of phenol, (b) Langmuir, (c) Freundlich and (d) Temkin adsorption isotherms to adsorb phenol onto the NMO/Al at room temperatures.

Various initial concentrations of phenol (50, 75, 100, 125 and 150 mg/L) were also used to examine the impact of initial concentration of phenol on adsorption by the NMO/Al. According to Figure 3a, adsorption capacity of phenol by the NMO/Al enhances when initial concentration of phenol increases. By increasing the initial concentration of phenol, the concentration gradient increases and acts as a driving force and as a result causes more absorption of phenol.[22] Clearly, adsorption procedure largely depends on contact time and initial concentration of phenol. Therefore, a contact time (60 minutes) and a C_0 (50 mg/L) can be chosen for other experiments.

Adsorption isotherm

To explain the adsorption capacities of phenol on the NMO/Al, the equilibrium experimental data was analyzed to assess the fitness of the data to the Langmuir, Freundlich, and Temkin isotherm models. The non-linear Langmuir isotherm model (Equation 4) is given below:[24]

$$q_e = \frac{Q_0 K_L C_e}{(1+K_L C_e)} \quad (4)$$

In Eq. 4, the equilibrium concentration of phenol (mg/L) has been denoted to Ce, the adsorbed phenol (mg/g) in the equilibrium time has been denoted to q_e, the monolayer adsorption capacity of NMO/Al nanocomposite has been denoted to Q_0 (mg/g) and the Langmuir constant has been denoted to K_L(L/mg).

The Langmuir model assumes that adsorption occurs on a homogeneous surface with a finite number of identical sites, and the adsorption of one molecule does not affect the adsorption of another. Using the linear form of Langmuir isotherm model (Equation 5), we can obtain the Langmuir isotherm variables.[24]

$$\frac{C_e}{q_e} = \frac{1}{Q_0 K_L} + \frac{C_e}{Q_0} \quad (5)$$

The plot of Ce/qe versus Ce is a straight line with a slope of $1/Q_0$ and an intercept of $1/Q_0K_L$. The values of Q_0 and K_L can be obtained from the slope and intercept of the linear plot, respectively (as shown in Fig. 3b).

According to Table I, the Langmuir isotherm parameters Q_0 and K_L were determined to be 53.2 mg/g and 0.034 L/mg, respectively, with a correlation coefficient (R) value of 0.9991. The highest monolayer adsorption capacity for phenol onto the NMO/Al at 298 K was found to be 53.2 mg/g. This suggests that the NMO/Al has a good adsorption capacity for removing phenol from the aqueous solutions.

Table I. The isotherm constants to adsorb phenol onto the surface of NMO/Al.

Isotherm models	constants	Value
Langmuir	Q (mg/g)	53.2
	K_L (L/g)	0.33
	R^2	0.9983
Freundlich	K_f (mg/g)	22.29
	1/n	0.222
	R^2	0.9844
Temkin	K_t (L/mol)	3.37
	B	17.81
	R^2	0.9888

The Freundlich isotherm is another empirical equation used to describe adsorption on a heterogeneous surface. It assumes that the adsorption occurs at sites with different adsorption energies, and the amount of adsorbate adsorbed increases with increasing of concentration. The linearized form of the Freundlich isotherm equation is given by Equation 6:[25]

$$log\, q_e = log\ \ K_f + \frac{1}{n}\ log\ \ C_e \quad (6)$$

where q_e is the amount of adsorbed phenol at equilibrium (mg/g), Ce is the equilibrium concentration of phenol (mg/L), K_f is the Freundlich constant related to the adsorption capacity (mg/g)*(L/mg)$^{(1/n)}$, and n is the Freundlich exponent related to the intensity of adsorption.

The plot of log (q_e) versus log (C_e) is a straight line with a slope of 1/n and an intercept of log(K_f). The values of n and K_f can be obtained from the slope and intercept of the linear plot, respectively (as shown in Figure 3c).

Table I presents the Freundlich isotherm parameters for the adsorption of phenol on the NMO/Al. The value of n, which is an experimental parameter, changes with the degree of inhomogeneity of the bonded phenol on the surface of adsorbent. The n value greater than 1 indicates the optimal adsorption. The value of K_f indicates the capacity of phenol adsorption. Additionally, the adsorption intensity will be more significant when the n-value is greater.[25]

The linear form of the Temkin isotherm is expressed by Equation 7:[25]

$$q_e = B\ ln\ K_t + B\ ln\ C_e \quad (7)$$

The adsorbate-adsorbent interactions considered by Temkin isotherm and assumes that the heat of adsorption decreases linearly with the covering the absorbent surface by the adsorbate substance. In Eq. 7, q_e and C_e have the same definitions as before, *B* refers to the Temkin constant associated with the adsorption heat, and K_t refers to the constant of equilibrium (L/mg).

The plot of q_e versus ln (C_e) is a straight line with slope of *B* and an intercept of *B* ln (K_t). *B* and K_t can be obtained from the slope and intercept of the resulting line, respectively. The linear plot of q_e versus ln (C_e) for the adsorption of phenol on NMO/Al was showed in Figure 3d.

Table I provides the Temkin constants and R^2 value for the adsorption of phenol on the NMO/Al. These constants give us information about the adsorption heat and maximum binding energy of the adsorbate on the adsorbent.

Table I indicates that the Langmuir model provides a better fit to the experimental data, as evidenced by its higher R^2 value. The maximum monolayer adsorption capacity for phenol on the NMO/Al was found to be 53.2 mg/g at 25°C. Since the value of n in the Freundlich equation (4.504) is between 1 and 10, therefore the absorption of phenol is favorable.[25]

Kinetic examination

To assesses of phenol adsorption kinetics on the NMO/Al, the intraparticle diffusion model (IPD), the Lagergren's pseudo-first and second-order models and the Elovich model were assessed. The pseudo-first order model (Equation 8) is as follows:[26]

$$ln\ (q_e - q_t) = ln\ q_e - K_1\ t \quad (8)$$

In Equation 8, q_t and q_e represent the amount of phenol adsorbed (mg/g) at any time t (min) and at equilibrium, respectively. K_1 is the rate constant of the

pseudo-first order sorption (min^{-1}). The value of q_e and K_1 can be determined from the intercept and the slope of the plot of $\log(q_e-q_t)$ versus t, as shown in Figure 4a.

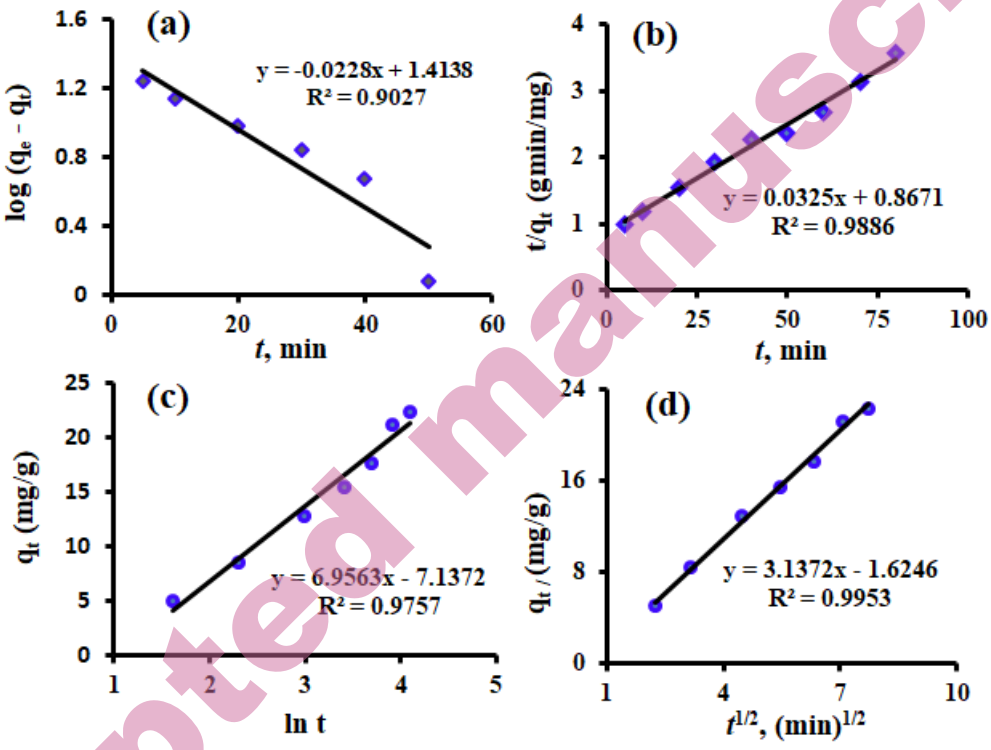

Fig. 4. The phenol adsorption kinetic onto the NMO/Al at room temperature: (a) pseudo first order, (b) pseudo second order, (c) Elovich and (d) intraparticle diffusions plots.

Pseudo second-order model is defined as follows (Eq. 9):[26]

$$\frac{dq_t}{dt} = k_2(q_e - q_t)^2 \quad (9)$$

Rearranging the variables gives (Eq. 10):

$$\frac{dq_t}{(q_e-q_t)^2} = k_2 dt \quad (10)$$

When equation 10 has been integrated in the boundary conditions t=0 (q=0) to t=t (q=qt), equation 11 has been obtained.

$$\frac{t}{q_t} = \frac{1}{K_2 q_e^2} + \frac{t}{q_e} \quad (11)$$

In the above equation, K2 represents the rate constant of pseudo-second order adsorption (g/mg min). The value of q_e and K_2 can be also calculated from slope and intercept of plot (t/qt versus t), as shown in Figure 4b.

The Elovich equation was also used to qualitatively describe the chemisorption process.[25] The linear form of the Elovich model is expressed by Equation 12:

$$q_t = \frac{1}{\beta} ln\, \alpha\, \beta + \frac{1}{\beta} ln\, t \quad (12)$$

In Equation 12, α (g/mg min) refers to the sorption rate and β (g/mg) refers to activation energy of chemisorption. Chemisorption is a process in which the adsorbate molecules are bonded to the surface of the adsorbent through chemical bonds. The sorption rate (α) represents the rate at which the adsorbate molecules are chemically bonded to the surface of the adsorbent. The activation energy (β) represents the minimum energy required for the adsorbate molecules to overcome the energy barrier and form chemical bonds with the adsorbent surface.

The values of α and β can be determined from the plot of q_t versus ln t, as shown in Figure 4c.

In the intraparticle diffusion model, the plot of q_t versus $t^{1/2}$ gives a straight line, which can be expressed by Equation 13:[26]

$$q_t = K_{id}\, t^{\frac{1}{2}} + C \quad (13)$$

In this equation, the rate constant of intraparticle diffusion (mg/g $min^{1/2}$) was denoted to K_{id} and the intercept of the line denoted to C (Figure 4d).

The resulted kinetic parameters from these models summarizes in Table II. The calculated q_e value for the Elovich model is in close agreement with the experimental q_e value, indicating a good fit of this model to the experimental data. The K_{id} for phenol was 3.14 mg/g $min^{1/2}$, which shows the high tendency of the NMO/Al for removal of phenol.[27]

NMO/Al reusability

Adsorbent reusability is a leading factor in the environmentally-friendly and economical process of adsorption. The problem with contaminated adsorbent disposal to the environment may be thus decreased due to adsorbent reusability. The results showed that the Re% of phenol in cycles 1 to 5 were 97.2, 94.7, 89.6, 85.1 and 80.3 respectively, that indicating the excellent reusability of NMO/Al.

Table II. Kinetics constants for phenol sorption onto the NMO/Al.

Kinetics model	Coefficients	Value
	q_e experimental (mg/g)	22.38
Pseudo first order	k_1 (1/min)	0.023
	q_e calculated (mg/g)	4.11
	R^2	0.9027
Pseudo second order	k_2 (g/mg min)	0.0012
	q_e calculated (mg/g)	30.77
	R^2	0.9886
Elovich model	α (mg/ g min)	19.40
	β (g/mg)	0.144
	q_e calculated (mg/g)	21.34
	R^2	0.9757
Intra-particle diffusion model	k_{id} (mg/g $min^{1/2}$)	3.14
	q_e calculated (mg/g)	22.7
	R^2	0.9953

Treatment of wastewater sample

The real wastewater samples were collected from an industrial center in Kerman Province, Iran, and then examined for the respective content using inductively coupled plasma-optical emission spectrometry (ICP-OES) as shown in Table III. In the next step, real wastewater samples were spiked with phenol (50 mg/L) and treated with the NMO/Al under optimized conditions. The mixture was then separated and analyzed for metal ion levels and phenol content using ICP-OES and spectrophotometer, respectively (Table III). The results showed that the NMO/Al was highly efficient in removing phenol and some metal ions from the wastewater samples.

Table III. Application of the NMO/Al to remove phenol from wastewater sample.

Metal ions	Concentration before treatment (mg/L)*	Concentration after treatment (mg/L)	Re (%)
phenol	50.0	3.2	93.6
Cr	5.3	0.6	88.7
Pb	5.4	0.7	87.0
Cu	8.1	0.8	90.1
Ni	6.2	0.9	85.5
Cd	4.5	0.5	88.9
Mn	4.3	Not detect	100
Co	5.2	Not detect	100
As	3.7	Not detect	100

*Original sample spiked with 50 mg/L of phenol.

CONCLUSION

In this study, a novel and effective adsorbent was developed by chemically depositing MnO_2 nanoparticles onto the surface of alumina. The results obtained from FT-IR, SEM, XRD, and XPS analyses confirmed the successful grafting of MnO_2 nanoparticles onto the alumina surface. The applicability of the NMO/Al as a new adsorbent was further confirmed by its ability to effective removal of phenol from an effluent sample. The Langmuir isotherm model well indicated the equilibrium data, and the highest phenol adsorption capacity on the NMO/Al was reported by 53.2 mg/g. The desorption experiment results showed that the NMO/Al adsorbent can be recovered and reused for up to five cycles. In the next works, the NMO/Al nanocomposite could be magnetized using iron oxide or cobalt oxide nanoparticles and then used to remove various contaminants from contaminated samples.

SUPPLEMENTARY MATERIAL

Additional data are available electronically at the pages of journal website: https://www.shd-pub.org.rs/index.php/JSCS/article/view/12633, or from the corresponding author on request.

Acknowledgement: The current study was conducted thanks to the support of Payame Noor University. The Bam University of Medical Sciences, Bam, Iran, provided financial assistance (project no. 98000075), which the authors gratefully thank"

И З В О Д

ПРИПРЕМА, КАРАКТЕРИЗАЦИЈА И ЕВАЛУАЦИЈА НАНО МАНГАН ДИОКСИДА КОЈИ ОБЛАЖЕ ГЛИНИЦУ, КАО НОВОГ АДСОРБЕНТА ЗА ЕФИКАСНО УКЛАЊАЊЕ ФЕНОЛА ИЗ ВОДЕНИХ УЗОРАКА

SAYED ZIA MOHAMMADI[1], FARIDEH MOUSAZADEH[2]*, LEILA SALAJEGHEH-TEZERJI[1], BATOUL LASHKARI[3], ELINA BANI-ASADI[2]

[1]Department of Chemistry, Payame Noor University, Tehran, Iran, [2]School of Public Health, Bam University of Medical Sciences, Bam, Iran, and [3]Department of New Materials, Institute of Science and High Technology and Environmental Sciences, Graduate University of Advanced Technology, Kerman, Iran

Ефикасан сорбент, нано-манган диоксид на нанокомпозиту глинице (NMO/Al) припремљен је као економичан адсорбент у овом раду. У том циљу, различитим техникама су одређене морфолошке, хемијске и површинске карактеристике NMO/Al. NMO/Al нанокомпозит се може без напора одвојити од узорака воде помоћу филтер папира, да би затим било процењено уклањање фенола из узорака отпадне воде. Сходно томе, испитани су различити емпиријски параметри који утичу на ово уклањање укључујући pH, јонску силу, време, температуру и концентрацију фенола. Да би се испитала адсорпциона равнотежа, коришћене су Langmuir, Freundlich, и Temkin једначине. Langmuir адсорпциони модел је имао већи коефицијент корелације (R^2), што указује на боље уклапање у карактеристике адсорпције. За процену кинетике адсорпције фенола на NMO/Al нанокомпозиту коришћени су различити кинетички модели. На основу резултата, Elovich модел је показао најбоље слагање са капацитетом сорпције од 21,34 mg g^{-1}. Додатно, адсорбовани фенол је ефикасно десорбован са NMO/Al површине коришћењем етанола, а

затим је NMO/Al нанокомпозит поново коришћен за уклањање фенола. Резултати су показали да се NMO/Al нанокомпозит може користити у више од пет циклуса. На основу налаза, процес адсорпције фенола из отпадне воде коришћењем NMO/Al нанокомпозита се сматра ефикасним адсорпционим приступом у систему адсорпције великих размера.

(Примљено 21. октобра 2023; ревидирано 14. новембра 2023; прихваћено 6. априла 2024.)

REFERENCES

1. Q. Yu, M. Tang, G. Liu, M. Liu, J. Ye, *Chem. Eng. Process* **186** (2023) 109313 (https://doi.org/10.1016/j.cep.2023.109313)
2. A.K. Mohammed, J.K. Ali, M.B.S. Kuzhimully, M.A. Addicoat, S. Varghese, M. Baias, E. Alhseinat, D. Shetty, *Chem. Eng. J.* **466** (2023) 143234 (https://doi.org/10.1016/j.cej.2023.143234)
3. P. Kazemi, M. Peydayesh, A. Bandegi, T. Mohammadi, O. Bakhtiari, *Chem. Eng Res Des.* **92**, (2014) 375 (https://doi.org/10.1016/j.cherd.2013.07.023)
4. F. Khoshtinat, T. Tabatabaie, B. Ramavandi, S. Hashemi, *Chemosphere* **283** (2021) 131265 (https://doi.org/10.1016/j.chemosphere.2021.131265)
5. S. Zarin, Z. Aslam, A. Zahir, M. Shahzad Kamal, A. Ghaffar Rana, W. Ahmad, S. Ahmed, *J. Iran. Chem. Soc.* **15** (2018)2689 (https://doi.org/10.1007/s13738-018-1457-1)
6. R. Sridar, U. Uma Ramanane, M. Rajasimman, *Environ. Nanotechnol. Monitor. Manag.* **10** (2018) 388 (https://doi.org/10.1016/j.enmm.2018.09.003)
7. K.A. Hernández-Hernández, J. Illescas, M.C. Díaz-Nava, S. Martínez-Gallegos, C. Muro-Urista, R.E. Ortega-Aguilar, E. Rodríguez-Alba, E. Rivera, *Appl. Clay Sci.* **157** (2018) 212 (https://doi.org/10.1016/j.clay.2018.01.020)
8. M. Mallek, M. Chtourou, M. Portillo, H. Monclús, K. Walha, A. ben Salah, V. Salvadó, *J. Environ. Manag.* **223** (2018) 576 (https://doi.org/10.1016/j.jenvman.2018.06.069)
9. X. Yang, X. Liu, W. Tang, Y. Gao, H. Ni, J. Zhang, *Korean J. Chem. Eng.* **34** (2017) 723 (https://doi.org/10.1007/s11814-016-0311-3)
10. S.Z. Mohammadi, Z. Darijani, M.A. Karimi, *J. Alloys Compd.* **832** (2020) 154942 (https://doi.org/10.1016/j.jallcom.2020.154942)
11. T. Pernyeszi, V. Farkas, A. Felinger, B. Boros, I. Dékány, *Environ. Sci. Pollut. Res.* **25** (2018) 8550 (https://doi.org/10.1007/s11356-017-1120-x)
12. N.S. Mirbagheri, S. Sabbaghi, *Microporous Mesoporous Mater.* **259** (2018) 134 (https://doi.org/10.1016/j.micromeso.2017.10.007)
13. Y. Yu, Z. Hu, Y. Wang, H. Gao, *Int. J. Miner. Process.* **162** (2017) 1 (https://doi.org/10.1016/j.minpro.2017.02.001)
14. M. Aazza, H. Ahlafi, H. Moussou, H. Maghat, *J. Environ. Chem. Eng.* **5**, (2017) 3418 (https://doi.org/10.1016/j.jece.2017.06.051)
15. C. di Luca, F. Ivorra, P. Massa, R. Fenoglio, *Chem. Eng. J.* **268** (2015) 280 (https://doi.org/10.1016/j.cej.2015.01.074)
16. E. Deschamps, V.S.T. Ciminelli, P.G. Weidler, A.Y. Ramos, *Clays Clay Miner.* 51 (2003) 197 (https://doi.org/10.1346/CCMN.2003.0510210)
17. S.M. Maliyekkal, A.K. Sharma, L. Philip, *Water Res.* 40 (2006) 3497 (https://doi.org/10.1016/j.watres.2006.08.007)

18. O.A. Elhefnawy, W.I. Zidan, M.M. Abo-Aly, E.M. Bakier, G.A. Al-Magid, *Spectrosc. Lett.* **47** (2014) 131 (https://doi.org/10.1080/00387010.2013.773519)
19. K. Atrak, A. Ramazani, S. Taghavi Fardood, *J. Mater. Sci. Mater. Electron.* **29** (2018) 8347 (https://doi.org/10.1007/s10854-018-8845-2)
20. X. Wan, S. Yang, Z. Cai, Q. He, Y. Ye, Y. Xia, G. Li, J. Liu, ***Nanomaterials*** **9** (2019) 847 (https://doi.org/10.3390/nano9060847)
21. S.Z. Mohammadi, H. Hamidian, L. Karimzadeh, Z. Moeinadini, *Arab. J. Chem.* **9** (2016) S1290 (http://dx.doi.org/10.1016/j.arabjc.2012.02.002)
22. Y.-D. Liang, Y.-J. He, T.-T. Wang, L.H. Lei, *J. Water Process Eng.* **27** (2019) 77 (https://doi.org/10.1016/j.jwpe.2018.11.013)
23. Y. Zhou, X. Liu, L. Tang, F. Zhang, G. Zeng, X. Peng, L. Luo, Y. Deng, Y. Pang, J. Zhang, *J. Hazard. Mater.* **333** (2017) 80 (https://doi.org/10.1016/j.jhazmat.2017.03.031)
24. S. Z. Mohammadi, Z. Safari, N. Madady, *J. Inorg. Organomet. Polym. Mater.* **30** (2020) 3199 (https://doi.org/10.1007/s10904-020-01485-x)
25. S. Z. Mohammadi, N. Mofidinasab, M. A. Karimi, A. Beheshti, *Int. J. Environ. Sci. Technol.* **17** (2020) 4815 (https://doi.org/10.1007/s13762-020-02767-0)
26. S. Z. Mohammadi, N. Mofidinasab, M. A. Karimi, F. Mosazadeh, *Water Sci. Technol.* **82** (2020) 829 (https://doi.org/10.2166/wst.2020.375)
27. S. Z. Mohammadi, M. A. Karimi, S. N. Yazdy, T. Shamspur, H. Hamidian, *Quim Nova* **37** (2014) 804 (https://www.scielo.br/j/qn/a/yGw8SYRs7w5ZdY7w6S4f4hR/?lang=en).